

1001

NRL Report 8519

# Toward an Understanding of the Turbulent Electrode Effect Over Land

J. C. WILLETT

*Environmental Sciences Division*

*Shelf  
4300*

September 29, 1981



**NAVAL RESEARCH LABORATORY**  
Washington, D.C.

Approved for public release; distribution unlimited.

Hogg [15], working in fields of the order of 400 V/m in the polluted atmosphere at Kew Observatory (typical total conductivity,  $0.2 \times 10^{-14}$  mho/m) and, according to Higazi and Chalmers [16], "in most cases in still air" reported that the positive polar conductivity decreased with height over the lowest meter while the negative component increased such that the total remained nearly constant with height. The space charge was positive, both at the surface and at 12.5 cm, and was nearly all on aerosol particles, but its magnitude was small enough that there was no significant variation of electric field with height, in contrast to Crozier's observations.

The decrease in  $\lambda_+$  with increasing height can be explained only by surface (or trapped) radioactivity, and the increase in  $\lambda_-$  with height, as well as the shallowness of the layer, suggests that the nonturbulent electrode effect is operative. It would appear that the situation observed by Hogg is similar to a case solved by Hoppel [3] in which ground radioactivity and significant aerosol density together confine the electrode effect to a thin layer and reduce the variation of electric field with height. This solution gives conductivity profiles of the type described but is applicable to extremely weak mixing which could be expected only under calm conditions without direct sunlight.

Hogg took great care to assure that his conductivity profiles were not distorted by the introduction of an elevated and grounded instrument into an ambient electric field. His approach of using varying lengths of cardboard tubing with their tops equalized by guard rings to the ambient potential, to extend the grounded Gerdien intakes from the surface to the desired height, was shown to cause only a small diffusional loss of ions to the tube walls. Hogg gives indications, however (in his section 3.A.d), that the field at the mouth of the intake tube may have a significant influence on the relative numbers of positive and negative ions entering. It would seem safer to equalize the Gerdien condenser itself to the ambient potential when making elevated measurements, so as to eliminate the strong axial field in the tube.

A number of experimenters have investigated the turbulent electrode effect in varying degrees of complexity. Over Greenland, where there is uniform ionization and negligible aerosol loading, Pluvinaige and Stahl [10] and Ruhnke [11] have shown that the conductivity ratio decreases toward unity with increasing wind speed. If the ratio data taken by the former workers at Station Centrale are plotted against wind speed  $u$ , which ranged from 1 to 7 m/s (with the plot excluding two points without wind data and two with excessive disagreement between the calculated and observed values of  $\lambda_+ - \lambda_-$ ), the linear relation  $\lambda_+/\lambda_- = 7.54 - 0.89u$  can be fitted with a correlation coefficient of  $-0.69$ , significantly different from zero at the 1% level. Furthermore Ruhnke's measurements suggest that at any level  $\lambda_-$  increases with wind speed. Except that neither paper gives evidence of a decrease in  $\lambda_+$  with increasing turbulence, both of these results are in agreement with the theoretical predictions of Hoppel [6] and myself [8]. With increasing wind speed at a given height, the negative-ion density should increase and the positive-ion density should decrease, as the classical electrode effect is destroyed, until they become approximately equal. Thereafter both ion densities should decrease due to a thickening of the layer over which turbulence transports ions to the surface.

Hoppel and Gathman [17] measured positive and negative conductivity alternately about 1 m above the tropical ocean where the aerosol density was  $2 \times 10^8$  to  $4 \times 10^8$   $\text{m}^{-3}$ . From the computed ion densities in their Table 1, and assuming  $q = 1.2 \times 10^6$   $\text{m}^{-3} \text{ s}^{-1}$ ,  $\alpha = 1.4 \times 10^{-12}$   $\text{m}^3 \text{ s}^{-1}$ ,  $Z = 3 \times 10^8$   $\text{m}^{-3}$ ,  $\beta_0 = 1.4 \times 10^{-12}$   $\text{m}^3 \text{ s}^{-1}$ , and  $\beta_1 = 4.0 \times 10^{-12}$   $\text{m}^3 \text{ s}^{-1}$  ( $\beta_0$  and  $\beta_1$  being combination coefficients between small ions and uncharged and oppositely charged nuclei respectively), we can calculate average values of  $n_+/n_\infty = 0.86$ ,  $n_-/n_\infty = 0.50$ , and  $n_+/n_- = 1.78$ , where  $n_\infty = 7.66 \times 10^8$   $\text{m}^{-3}$  is the equilibrium ion density under these conditions. The electric-field magnitude and bulk-aerodynamic eddy-diffusion coefficient at 1 m during these measurements

averaged 151 V/m and  $0.080 \text{ m}^2 \text{ s}^{-1}$ , so the closest numerical solution ( $E_0 = 150 \text{ V/m}$ ,  $\kappa(1 \text{ m}) = 0.59 \text{ m}^2 \text{ s}^{-1}$ , and  $Z = 0$ ) gives  $n_+/n_\infty \approx 0.94$ ,  $n_-/n_\infty = 0.51$ , and  $n_+/n_- = 1.85$ . Since the addition of a small concentration of nuclei in other model calculations of Hoppel and Gathman [7] has been shown to reduce  $n_+/n_\infty$  and  $n_-/n_\infty$  somewhat (by thickening the electrode layer) without much change to  $n_+/n_-$ , this can be regarded as good agreement. However, again no pains were taken to equalize the conductivity instrumentation to the ambient potential.

Measurements over land are made more difficult to interpret by nonuniform ionization and significant aerosol concentrations. Adkins [18], working in the clear air at Cavendish Laboratory, observed that in fields larger than 500 V/m (but not high enough for corona) the density of the upward-moving ions (measured with an ion counter 110 cm above the ground) was reduced, suggesting that the classical electrode effect can overpower the complications of turbulence, aerosol particles, and radioactivity if the fields are strong enough. Law [19], also at Cavendish but working in fields weaker than 100 V/m, found that the density of both positive and negative small ions decreased with increasing height in the lowest 1 m over short grass. This decrease was more pronounced at night than in daytime and can probably be explained in terms of surface and trapped radioactivity, as long as the turbulent mixing was not too strong. Neither Adkins nor Law appears to have equalized his instrumentation, although Law at least was aware of the potential problems.

Law also measured the space-charge density at a height of about 50 cm, finding that it reversed sign from negative at night to positive by day. In a nonturbulent atmosphere, for the conduction-current density to be nondivergent when a downward electric field is imposed on a region of downward conductivity gradient, a negative space charge is required in the steady state. This is clearly inconsistent with the daytime measurements, and Law showed that, even at night, the negative charge density was too small to be in equilibrium with the observed fields and ion-density profiles. The additional evidence that the electric field at Cavendish did not change much with height completes his convincing argument for the existence of convection currents, stronger by day but still acting at night, supplying positive charge at the 50-cm level by convergence.

Crozier [13] showed that the reversed electrode effect observed at his New Mexico site on calm nights was destroyed by a wind of 1 m/s or more. Hoppel [6] showed that this observation could be explained in his model by a combination of reduced radon trapping and increased turbulent mixing. Therefore both Crozier's and Law's measurements show the effects of weak turbulence in transporting positive charge, produced in the lowest 10 to 20 cm by the classical electrode mechanism, upward to neutralize or reverse the negative charge deposited above by convergence of the conduction current.

In an effort to resolve the apparent disagreement between the near-uniform profile of conductivity observed by Hogg at Kew [15] and the decrease of conductivity with increasing height implied by Law's measurements at Cavendish [19], Higazi and Chalmers [16] repeated some of Hogg's work at Durham, under conditions closer to those in Law's experiment. Typical values of total conductivity and electric field at Durham were  $1.1 \times 10^{-14} \text{ mho/m}$  and 115 V/m respectively, and the results were in general agreement with those of Law. Both the positive and the negative polar conductivities decreased with increasing height over the lowest meter, and the conductivity ratio  $\lambda_+/\lambda_-$  at the surface was always greater than unity. Furthermore both the slope of the profiles and the magnitude of the ratio decreased systematically with increasing wind speed.

Although the conductivity ratio at the ground shows the expected behavior with wind speed, the observed decrease in both polar conductivities with height, even at winds as high as 10 m/s, contradicts the theoretical results of Hoppel and, even more so, my results. One is tempted to blame this disagreement on surface radioactivity, which can cause a nonuniform ionization profile, even when the radon gas is well mixed, due to the short range of alpha and beta particles emitted by radioactive materials on the surface.

To estimate the effect of these emissions, we can compare the rate at which positive and negative ions are expected to diffuse to the ground, according to my theory, with the pair-production rate due to surface radioactivity. The latter has been estimated by Hoppel [3] as

$$q'(z) = \left[ 4.8e^{-2.36z} + 50 \tanh \left( \frac{8 \times 10^{-8}}{z^4} \right) \right] \times 10^6,$$

where the first term represents beta ionization and the second term corresponds to alpha particles. Vertical integration of this formula from the surface to height  $h$  yields 1.87, 2.93, and  $3.13 \times 10^6$  pairs/m<sup>2</sup> s for  $h = 20$  cm,  $h = 1$  m, and  $h \rightarrow \infty$  respectively.

The diffusive flux  $F$  of ions to the surface can be calculated from the simplified model developed in the next two sections of this report. Using the approximate expression for ion density implied by Eqs. (1) and (2) from these next two sections, we get

$$F = -\kappa(z) \frac{dn}{dz} = \frac{Kn_\infty}{2 \ln 2\sqrt{z_0/L}},$$

where  $n_\infty$  is the equilibrium ion density far from the surface,  $z_0$  is the roughness height, and  $L$  is the height scale of the profile. This diffusive flux is constant over the lowest few centimeters. Assuming a typical value of  $n_\infty = 3.0 \times 10^8$  m<sup>-3</sup> and taking the other parameter values from Table 3 in the next section, we obtain  $F = -7.5 \times 10^6$  and  $-4.5 \times 10^6$  ions/m<sup>2</sup> s for roughness heights  $z_0 = 1$  cm and 2 mm respectively.

These calculations indicate that the ionization due to surface radioactivity is too small to balance the diffusive flux to the surface, even if the former is integrated over the entire ionized layer. If a uniform background of radon, surface-gamma-ray, and cosmic-ray ionization of  $10^7$  pairs/m<sup>3</sup> s is included, the total ionization below about 50 cm is still too small (even neglecting ion losses due to recombination and aerosol attachment), requiring the turbulent ion transport at that level to be downward, or the ion-density gradient to be upward. It is therefore difficult to explain the decrease in conductivity with height observed by Higazi and Chalmers [16] in this way. It remains either to question the concept, central to the theories, that ions diffuse to an absorbing lower boundary or to doubt experimental results that appear quite unimpeachable.

Other observations from Durham, however, seem to support the theoretical models impugned above. Aspinall [20] concluded from surface measurements of the total conductivity, electric field, and total current (to a flush-mounted Wilson plate covered with natural sod) that the current density at the ground was made up of a conduction component averaging  $-1.07$  pA/m<sup>2</sup> and a convection component averaging  $-0.95$  pA/m<sup>2</sup>, both downward. Although the conduction current showed little diurnal variation, the convection current appeared to vary  $\pm 0.4$  pA/m<sup>2</sup>, in nearly perfect correlation with the diurnal variation of space-charge density measured at 80 cm. The space charge itself was always positive, with a maximum at night and minimum in the afternoon. These results suggest that space charge is being transported down its gradient to the surface by turbulent diffusion, as demanded by the theories of Hoppel and of myself.

Aspinall's conclusions could be questioned by two counts. First, he deduced the "surface field" from measurements with an inverted mill at 1 m. Although the measured space-charge densities were fairly low, there is always some uncertainty in reducing such a measurement to a definite height, as pointed out by Gathman and Trent [21]. Second, he calculated the "surface conduction-current density" from the polar conductivities measured in air aspirated through intakes flush with the ground. Since this air probably came from a layer at least 10 cm thick, there would have been

a systematic error in  $\lambda$  if the conductivities changed with height. If they increased with height, as I predicted [8], the resulting underestimate of the surface convection current makes the observations more compatible with the theoretical prediction that *all* the current there is carried by diffusion. If on the other hand the polar conductivities decreased with height, as found by Higazi and Chalmers [16], the convection current was overestimated and could have been negligible. This question can be settled only by further measurements.

### CONDUCTIVITY-PROFILE EXPERIMENT

In an effort to test my theoretical predictions and to clarify the nature of conductivity profiles and convection currents in the turbulent electrode layer, I carried out two experiments at the Waldorf Annex of the Naval Research Laboratory, an atmospheric electricity observatory previously described by Anderson and Dolezalek [22]. The first experiment was designed to measure profiles of polar conductivity over grass at various wind speeds. Four Gerdien chambers were mounted on a wooden tower as shown in Fig. 1, two resting on an aluminum plate on the ground, one at a height of 1 m, and one at 5 m. The uppermost sensor and the top of the tower were equalized to the ambient potential by means of a voltage-follower system described briefly by Gathman [23] and in more detail by Gathman and Trent [24]. The middle sensor, although isolated from ground, was found to float at only a few volts and can be considered at ground potential. The lowest two sensors, and the Obolensky space-charge filter mounted beside them, were grounded. The wind speed and direction at 5 m elevation were measured on another tower.

Cylindrical Gerdien tubes constructed of stainless steel were used in this experiment. A central electrode 12.7 mm (1/2 in.) in diameter and 20.3 cm (8 in.) long was held at instrument ground



Fig. 1 — Apparatus for the conductivity-profile experiment. The windward (near) tower supports Gerdien chambers 5 m and 1 m above the two Gerdien and the Obolensky filter on the ground. The radioactive probe for the potential equalizing system is mounted at the top of the leeward (far) pole. The white box at the left contains batteries for accelerating voltage and isolation amplifiers.

potential by a Philbrick 1702 parametric operational amplifier configured as a current amplifier. This probe was mounted concentrically inside an accelerating electrode 40.6 cm (16 in.) long with a 9.84 cm (3-7/8-in.) inside diameter to which approximately  $\pm 48$  V was supplied by batteries. The measured capacitance between probe and accelerating cylinder in this configuration was  $6.06 \text{ pF} \pm 1\%$ , and the aspiration rate was estimated at  $0.02 \text{ m}^3/\text{s}$ , giving a critical mobility of about  $6 \times 10^{-4} \text{ m}^2/\text{V s}$ .

These instruments were operated with an overall sensitivity of about  $4.3 \text{ V per } 10^{-14} \text{ mho/m}$ , each being calibrated to an accuracy of  $\pm 2\%$ . However, this uncertainty does not take into account errors due to partial truncation of the ion spectrum at the high-mobility end or to the turning away of ions by the accelerating field at the intake. A current-voltage characteristic of one of the chambers was plotted for negative ions in ambient laboratory air having a polar conductivity of  $0.92 \times 10^{-14} \text{ mho/m}$ . This curve began to deviate from a straight line for accelerating voltages greater than  $20 \text{ V}$  and indicate an underestimate of the conductivity by about  $6\%$  at  $50 \text{ V}$ .

The Obolensky filter used to measure space charge at the lowest level has been described by Anderson [25]. The current collected by an insulated tube filled with steel wool and absolute filters and aspirated at  $2.1 \times 10^{-2} \text{ m}^3/\text{s}$  was measured with another Philbrick 1702 operational amplifier. The overall sensitivity of this instrument was  $0.21 \text{ V per pC/m}^3 \pm 10\%$ .

The conductivity-profile experiment was carried out during the spring of 1977. Periods when the wind was from an acceptable direction, giving a fairly uniform surface of grass over an unobstructed upwind fetch of about  $100 \text{ m}$ , were divided into experimental runs. During each run one Gerdien tube at each level measured a given polarity of conductivity, the fourth instrument (at the lowest level) measuring the opposite polarity. Between runs the drift of all instruments was checked by stopping the aspiration of the Obolensky filter and zeroing the accelerating voltages of the Gerdien tubes. This permitted linear trends to be fitted to the zero drifts of the electronics so that they could be removed from the data.

All data were recorded once a second by a digital data-acquisition system after analog and numerical filtering to control aliasing. Table 1 shows the averages for each run, ranked in order of decreasing wind speed, after zero correction and application of calibration factors. All runs except the last two were during the daytime in weather ranging from cool and clear to hot and humid with variable cloudiness. The two runs at the lowest wind speeds occurred after sunset. The sign of the conductivity readings indicates the polarity of conductivity being measured. The lowest level has been arbitrarily assigned a height of  $20 \text{ cm}$  above the surface, this being a reasonable upper bound on the height from which air entering its instruments could have come.

Superficial examination of the data in Table 1 is facilitated by the first four rows in the bottom section, which give averages over all runs for which the uppermost Gerdien tube measured positive polar conductivity ( $\lambda_+$  runs), averages over all runs when the uppermost tube measured negative conductivity ( $\lambda_-$  runs), overall averages of all runs regardless of polarity, and standard deviations around these overall averages. Finally, in the last three rows, Student's  $t$  parameters expressing the differences between the first two averages in each column are given to allow the significance of these differences to be assessed.

Since we will be primarily interested in comparing the shapes of the polar-conductivity profiles, it is reassuring to note several features of these data. First, the conditions seem to be relatively stationary between the set of eleven  $\lambda_+$  runs and the set of six  $\lambda_-$  runs: average wind speeds for the  $\lambda_+$  and  $\lambda_-$  runs are similar, and average pole-top potentials and space-charge densities each differ by only  $13\%$ . Furthermore, the magnitudes of the mean positive and mean negative polar conductivities at the uppermost ( $5\text{-m}$ ) level are nearly identical. These features suggest that any differences detected between the mean conductivity profiles should not be dismissed on the grounds that the

two data sets were chosen from different populations. Second, there do appear to be real differences between profiles. For example, although the individual mean polar conductivities at the lowest level (0.2 m) show excellent agreement between the two sets of runs (respecting the opposite polarity of the measurements by the two instruments), there is a difference between  $\lambda_+$  and  $\lambda_-$  at 20 cm which is significant at the 5% level for one of the Gerdien tubes ( $\lambda_{2A}$ ) and at the 1% level ( $t = 3.04$ , 28 degrees of freedom) when both data sets are combined respecting measurement polarity.

Unfortunately, as with many meteorological data, there is enough variability among runs that averages of the sort discussed tend to obscure, rather than to illuminate, the behavior of the profiles. This variability manifests itself in Table 1 in the form of large standard deviations about the overall averages (coefficient of variation 20 to 50%) and is due primarily to two factors. The first is run-to-run change in meteorological conditions such as wind speed (measured) or aerosol density (not measured). Insofar as variance can be ascribed to changes in measured parameters, substantive conclusions result, but variance due to unmeasured parameters must be eliminated as much as possible. A second and more troublesome cause of variability among run averages is the existence of secular trends during runs, increasing the uncertainty in the individual averages.

A detailed examination of the time series during several runs has led to an artifice for reducing the effect of secular trends. It was observed that a substantial fraction of the total variance of polar conductivity at a given level belonged to the lowest frequencies. Even after removal of the linear trend, which typically accounted for around 30% of the variance, spectral analysis indicated integral time scales of the order of 70 s. Furthermore, the slow variations in conductivity at different levels tended to parallel one another.

It was found that a new time series constructed of the ratio of the instantaneous conductivity measured at one of the lower levels to that at 5 m behaved much better. Only about 4% of the total variance of such a ratio time series belonged to the linear trend, and the integral scale was more like 15 s. The conclusion was that the uncertainty in averages of these ratios was comparable to the instrument calibration accuracy of  $\pm 2\%$ , as compared with a typical uncertainty of about 9% in averages of raw conductivity over a run. Therefore attention will be confined to run averages of these conductivity ratios in what follows. An additional benefit of this procedure is the removal of some of the influence of unmeasured variables such as aerosol density.

The ratio data for selected runs are listed in Table 2. Omitted are four runs for which data from one of the Gerdien tubes was missing and two more whose representativeness could be questioned because of anomalously low charge-density measurements. The ratios tabulated in columns 6 through 8 are identified by the two conductivities involved; for example  $\lambda_{2A}/\lambda_5$  is the average of the ratio of the polar conductivity measured by the first of the two instruments at 20 cm to that measured by the one at 5 m (refer to the headings in Table 1). The signs of these ratios indicate the polarity of the conductivity in the numerator only. Column 9 in the table expresses the magnitude of negative polar conductivity relative to the positive polar conductivity at the 20-cm level.

Averages for the columns are presented in the first three rows in the lower section. Given in the last four rows are two kinds of Student's  $t$  values to facilitate estimates of the statistical significance of these averages: the  $t$  values labeled " $t_+$ ," " $t_-$ ," and "overall  $t$ " measure the departures from unity of the magnitude of the averages for the  $\lambda_+$  runs, the  $\lambda_-$  runs, and all runs respectively. The  $t$  values labeled "difference  $t$ " measure the difference between the magnitudes of the averages for  $\lambda_+$  runs and  $\lambda_-$  runs, as in Table 1. Those  $t$  values significant at the 1% level have been enclosed in boxes.

Profiles of the magnitudes of the conductivity ratios have been plotted in Fig. 2. The runs have been arbitrarily separated into six groups:  $\lambda_+$  runs and  $\lambda_-$  runs with wind speed less than 2.5,

Table 1 — Average data for each run in the 1977 conductivity-profile experiment. The sign of the conductivity in columns 7 through 10 refers to the polarity of ions being collected. The  $t$  value enclosed in the box is significant at the 5% level.

Run	Date (1977)	Length (min)	Wind Speed (m/s)	Pole-Top Potential (kV)	Space Charge ( $\mu\text{C}/\text{m}^3$ )	Polar Conductivities ( $10^{-14}$ mho/m)			
						$\lambda_5$ (5 m)	$\lambda_1$ (1 m)	$\lambda_{.2A}$ (0.2 m)	$\lambda_{.2B}$ (0.2 m)
1	May 1	38½	4.02	0.498	—	0.394	0.473	0.419	-0.386
2	May 1	45	3.87	0.330	1.5	-0.319	-0.345	-0.305	0.341
3	Apr. 28	25	3.81	0.321	12.5	0.615	0.659	0.522	-0.531
4	Apr. 28	39	3.78	0.446	14.1	0.629	0.693	0.600	-0.501
5	May 1	35	3.73	0.423	—	0.525	0.607	—	0.511*
6	Apr. 28	38	3.63	0.319	17.4	-0.658	-0.653	-0.488	0.583
7	May 6	47½	3.62	0.767	20.1	-0.633	-0.553	-0.400	0.613
8	Apr. 28	49	3.44	0.469	13.5	-0.633	-0.618	-0.474	0.570
9	May 1	44	3.42	0.344	-3.2	0.325	0.397	0.337	-0.357
10	May 6	44½	3.31	0.599	17.9	0.721	0.805	0.604	-0.497
11	May 6	43	3.29	0.444	15.9	-0.716	-0.677	-0.496	—
12	May 6	36½	3.26	1.036	25.5	0.706	0.783	0.621	—
13	May 6	22	3.12	0.552	20.7	0.868	0.951	0.723	—
14	Apr. 28	42½	3.09	0.523	15.6	0.571	0.649	0.540	-0.466
15	May 8	37½	2.48	0.619	14.0	0.410	0.519	0.414	-0.320
16	May 8	49½	2.11	0.602	16.3	-0.471	-0.451	-0.326	0.494
17	May 8	20	1.01	0.768	27.3	0.506	0.622	0.545	-0.369
Average, $\lambda_+$ runs			3.18	0.557	16.0	0.570	0.651	0.536	-0.428
Average, $\lambda_-$ runs			3.33	0.489	14.1	-0.572	-0.550	-0.415	0.520
Overall average			3.23	0.533	15.3	0.571	0.615	0.490	0.464
Overall std. dev.			0.75	0.190	7.8	0.152	0.153	0.118	0.099
$t$ value†			—	—	—	-0.021	1.34	<u>2.22</u>	1.76
Degrees of freedom†			—	—	—	15	15	14	11
5% level†			—	—	—	2.13	2.13	2.15	2.20

\*This value is positive because the instrument polarity was set to provide a substitute value for the missing  $\lambda_{.2A}$  value.

†Test of the difference of the average of the  $\lambda_+$  runs and the average of the  $\lambda_-$  runs.

Table 2 — Average conductivity ratios (referred to the uppermost level) for selected runs. The sign of the ratio refers to the polarity of the numerator only. The notation  $\lambda_{.2-}$  indicates a negative polarity measured by either  $\lambda_{.2A}$  or  $\lambda_{.2B}$ . The  $t$  values enclosed in boxes are significant at the 1% level.

Run	Wind Speed (m/s)	Pole-Top Potential (kV)	Space Charge ( $\mu\text{C}/\text{m}^3$ )	Polar Conductivity $\lambda_5$ (5 m) ( $10^{-14}$ mho/m)	Ratio Conductivities*			$\frac{\lambda_{.2-}/\lambda_5}{\lambda_{.2+}/\lambda_5}$ (20 cm)	$\lambda_{.2+}/\lambda_5$ (20 cm)	$\lambda_{.2-}/\lambda_5$ (20 cm)	$ \lambda_1/\lambda_5 - \lambda_{.2A}/\lambda_5 $	
					$\lambda_1/\lambda_5$ (1 m)	$\lambda_{.2A}/\lambda_5$ (20 cm)	$\lambda_{.2B}/\lambda_5$ (20 cm)				$\lambda_+$ Runs	$\lambda_-$ Runs
1	4.02	0.498	—	0.394	1.194	1.067	-0.972	0.911	—	—	0.127	—
3	3.81	0.321	12.5	0.615	1.073	0.854	-0.866	1.014	—	—	0.219	—
4	3.78	0.446	14.1	0.629	1.109	0.963	-0.802	0.833	—	—	0.146	—
6	3.63	0.319	17.4	-0.658	-0.997	-0.746	0.891	0.837	—	—	—	0.251
7	3.62	0.767	20.1	-0.633	-0.874	-0.639	0.978	0.653	—	—	—	0.235
8	3.44	0.469	13.5	-0.633	-0.980	-0.750	0.907	0.827	—	—	—	0.230
10	3.31	0.599	17.9	0.721	1.121	0.842	-0.694	0.824	—	—	0.279	—
14	3.09	0.523	15.6	0.571	1.141	0.950	-0.822	0.865	—	—	0.191	—
15	2.48	0.619	14.0	0.410	1.276	1.017	-0.793	0.780	—	—	0.259	—
16	2.11	0.602	16.3	-0.471	-0.961	-0.701	1.053	0.666	—	—	—	0.260
17	1.01	0.768	27.3	0.506	1.250	1.100	-0.749	0.681	—	—	0.150	—
Av, $\lambda_+$ runs	3.07	0.539	16.9	0.557	1.166	0.970	0.814	—	—	—	0.196	—
Av, $\lambda_-$ runs	3.20	0.539	16.8	-0.599	-0.953	-0.709	0.957	—	—	—	—	0.244
Overall av	3.12	0.539	16.9	0.574	—	—	—	0.808	0.966	-0.776	—	—
$t_+$	—	—	—	—	5.80	-0.79	-5.56	—	—	—	—	—
$t_-$	—	—	—	—	-1.72	-11.3	-1.15	—	—	—	—	—
Overall $t$	—	—	—	—	—	—	—	-5.82	-1.31	-8.16	—	—
Difference $t$	—	—	—	—	4.90	4.84	2.72	—	—	—	4.16	6.48

\*Averages of the indicated ratios of measured polar conductivities, as described in the text.

between 2.5 and 3.5, and greater than 3.5 m/s. Each profile is labeled with its mean wind speed and plotted relative to a value of 1.0 at 5 m. The three ratios of the same polarity are connected with line segments, and the fourth ( $\lambda_+ 2B/\lambda_5$ , with a negative polarity for  $\lambda_+$  runs and a positive polarity for  $\lambda_-$  runs) is plotted separately using the same symbol.

Before discussing the significance of these profiles, I reemphasize that the Gerdien instrument at the 1-m level was not equalized and hence floated near ground potential. An imbalance of the order of -100 V generally existed between it and the ambient atmosphere, and the data at 1 m should therefore be viewed with skepticism. Such an imbalance would be expected to cause some underestimation of the negative polar conductivity, due to the repulsion of negative ions from the intake, but to have little effect on the measurement of the positive component. Consequently it is hard to explain away the highly significant maximum of  $\lambda_+$  observed at that level by this mechanism. One might even suspect the existence of a similar, though smaller, maximum in the true negative conductivity at 1 m as well.

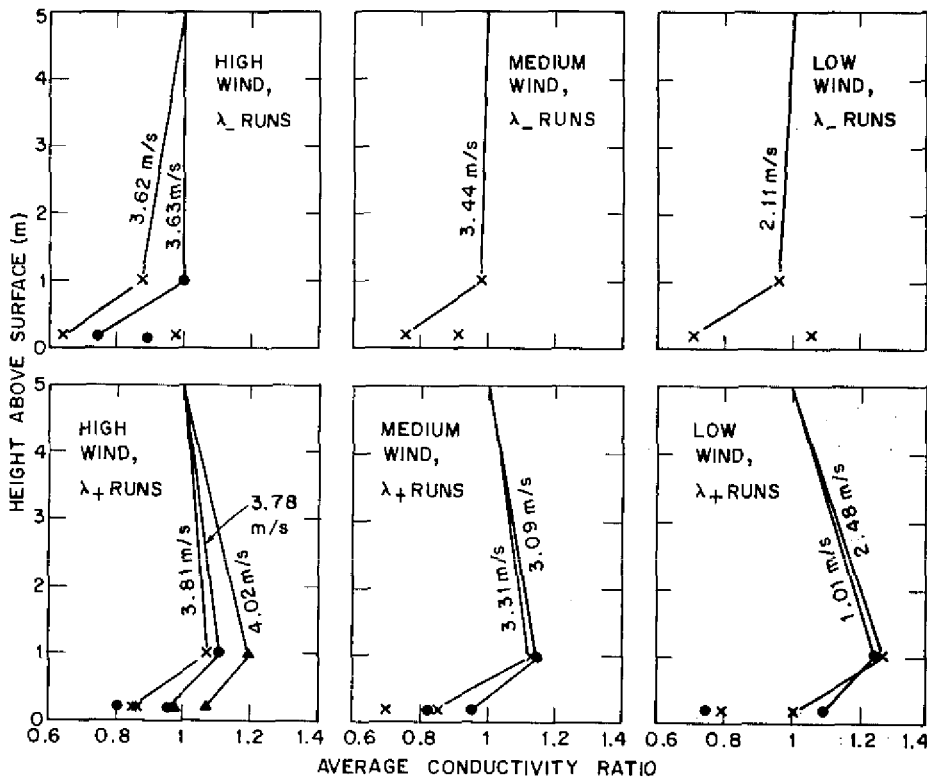


Fig. 2 — Profiles of the magnitudes of the average conductivity ratios. The runs have been separated into three columns according to wind speed (with which each profile is labeled in meters per second) and into two rows according to the polarity of the conductivity measured by three of the four Gerdien tubes. The four data points for each profile are plotted with a common symbol, with the three of the same polarity being connected by line segments.

The picture emerging from Table 2 and Fig. 2 depends on whether or not the measurements at the 1-m level are accepted. If so, then *both* polar conductivities strongly increase with height in the lowest meter (indicated in the last two columns of Table 2), in agreement with my [8] conclusion that ions diffuse to the surface, where they are annihilated. The observed decrease in  $\lambda_+$  from 1 m to 5 m must be explained in terms of greatly increased ionization in the lowest few meters, perhaps caused by  $\beta$  emission from the surface. The classical electrode effect is clearly felt at 20 cm, where  $\lambda_-/\lambda_+$  is significantly less than unity. Because of possible underestimation of  $\lambda_-$  at 1 m, however, it is difficult to say whether  $\lambda_-$  is really less than  $\lambda_+$  there or not.

If this view of the situation is correct, one would expect  $\lambda_-/\lambda_+$  at 20 cm to increase toward unity and both  $\lambda_+$  and  $\lambda_-$  at 1 m to decrease relative to their values at 5 m, as the wind speed increases and the conductivity profiles become dominated by turbulent mixing. Although the range of wind speeds obtained in this experiment was not very great, a correlation coefficient of +0.63, significantly different from zero at the 5% level, was indeed found between the ratio  $|(\lambda_-/\lambda_+)/(1.2/\lambda_5)|$  and the wind speed. No relationship was found between  $\lambda_-$  at 1 m and wind speed; but the correlation between  $\lambda_1/\lambda_5$  and wind speed for  $\lambda_+$  runs, though not statistically significant, measured -0.70 in accordance with theory.

If, on the other hand, the conductivity measurements at 1 m are completely excluded from consideration, we are left with only the strong increase in  $\lambda_-$  from 20 cm to 5 m. This could be explained by the classical electrode effect without recourse to the annihilation of ions at the surface. Combining all measurements of  $\lambda_+$  at 20 cm leads to an average  $\lambda_{.2+}/\lambda_5$  (column 10 in Table 2) somewhat less than unity and a correlation coefficient of -0.59 with wind speed, but neither of these statistics is significant at the 5% level.

For comparison with the above experimental results, I have derived a theoretical ion-density profile. Since the height scale of this profile can be substantially decreased by the effect of aerosol attachment on the small-ion lifetime, I decided not to use the profiles in Ref. 8 directly. Instead, I made the following four assumptions: my conclusion that the profiles of polar ion density become similar and independent of the electric field in a limit of strong turbulence remains valid, my lower-boundary condition that the mean ion density vanishes at the roughness height  $z_0$  over an aerodynamically rough surface also remains valid, aerosol attachment replaces recombination as the dominant ion-loss process (true over land for  $Z > 5 \times 10^9 \text{ m}^{-3}$ ), and a simple linear model can be used for the aerosol attachment rate (true if the electric field and charge density are not too large).

Using an eddy-diffusion model for the turbulent flux of ions, I obtained an equation for the small-ion density  $n$  in the steady state:

$$-K \frac{d}{dz} z \frac{d}{dz} n = q - \beta n Z,$$

where  $K$  is a constant proportional to wind speed, as I introduced on page 4, and  $\beta$  is the effective aerosol attachment coefficient. This equation has the solution

$$n(z) = n_\infty \left[ 1 - K_0(2\sqrt{z/L})/K_0(2\sqrt{z_0/L}) \right], \quad (1)$$

where  $n_\infty \equiv q/\beta Z$  is the equilibrium ion density far from the surface,  $L \equiv K/\beta Z$  is the height scale of the profile, and  $K_0(w)$  is the modified Bessel function of the second kind, order zero, of the argument  $w$ . Results computed from this solution are given in Table 3 for a mean wind speed at 5 m of 4 m/s and two values of the roughness height. The friction velocity  $u_*$  has been estimated from the logarithmic wind profile at neutral stability, and I have taken  $K = 0.47u_*$ , following my earlier analysis [8]. Assumed values of  $q = 10^7 \text{ m}^{-3} \text{ s}^{-1}$ ,  $Z = 2.1 \times 10^{10} \text{ m}^{-3}$ , and  $\beta = 1.6 \times 10^{-12} \text{ m}^3/\text{s}$

REPORT DOCUMENTATION PAGE		READ INSTRUCTIONS BEFORE COMPLETING FORM	
1. REPORT NUMBER NRL Report 8519	2. GOVT ACCESSION NO.	3. RECIPIENT'S CATALOG NUMBER	
4. TITLE (and Subtitle) TOWARD AN UNDERSTANDING OF THE TURBULENT ELECTRODE EFFECT OVER LAND		5. TYPE OF REPORT & PERIOD COVERED Interim report on a continuing NRL problem.	
		6. PERFORMING ORG. REPORT NUMBER	
7. AUTHOR(s) J.C. Willett		8. CONTRACT OR GRANT NUMBER(s)	
9. PERFORMING ORGANIZATION NAME AND ADDRESS Naval Research Laboratory Washington, DC 20375		10. PROGRAM ELEMENT, PROJECT, TASK AREA & WORK UNIT NUMBERS 61153N RR033-02-42 43-1106-0-1	
11. CONTROLLING OFFICE NAME AND ADDRESS Office of Naval Research Arlington, VA 22217		12. REPORT DATE September 29, 1981	
		13. NUMBER OF PAGES 31	
14. MONITORING AGENCY NAME & ADDRESS (if different from Controlling Office)		15. SECURITY CLASS. (of this report) UNCLASSIFIED	
		15a. DECLASSIFICATION/DOWNGRADING SCHEDULE	
16. DISTRIBUTION STATEMENT (of this Report)  Approved for public release; distribution unlimited.			
17. DISTRIBUTION STATEMENT (of the abstract entered in Block 20, if different from Report)			
18. SUPPLEMENTARY NOTES			
19. KEY WORDS (Continue on reverse side if necessary and identify by block number) Electrode effect                      Electrical conductivity Atmospheric electricity Turbulent transport Surface layer Convection current			
20. ABSTRACT (Continue on reverse side if necessary and identify by block number) A new concept of the turbulent electrode effect, which has emerged from the recent work of Hoppel and of the author, is described. The past theoretical and observational research relating to the transformation of the "classical electrode layer" in the case of strong turbulent mixing is reviewed. Results of two experiments designed to test key predictions of the new theories are reported. The first experiment, measurement of the conductivity profile over land on windy days, lends some support to the theoretical prediction that both the positive and the negative polar components of the atmospheric conductivity should decrease toward the surface under turbulent conditions. The second experiment, <p style="text-align: right;">(Continues)</p>			

Table 3 — Computed ion-density ratios based on a 5-m wind speed of 4m/s,  
for two values of roughness length  $z_0$

Roughness Height $z_0$ (cm)	Friction Velocity $u_*$ (m/s)	Diffusion Constant $K$ (m/s)	Height Scale $L$ (m)	Ion-Density Ratios		Ratio Difference	
				$\frac{n(1\text{ m})}{n(5\text{ m})}$	$\frac{n(20\text{ cm})}{n(5\text{ m})}$	$\frac{n(1\text{ m})}{n(5\text{ m})} - \frac{n(20\text{ cm})}{n(5\text{ m})}$	
1.0	0.23	0.11	3.2	0.869	0.618	0.252	
0.2	0.18	0.085	2.5	0.915	0.735	0.181	

(calculated from  $\beta = 2\eta_1/(2 + \eta_1/\eta_0)$  with  $\eta_1 = 4 \times 10^{-12}$  m<sup>3</sup>/s and  $\eta_0 = 1.4 \times 10^{-12}$  m<sup>3</sup>/s, as before) imply  $n_\infty = 3.0 \times 10^8$  m<sup>-3</sup>, in agreement with the average total conductivity at 5 m during the experiment.

The value of  $z_0 = 1$  cm used in Table 3 was intended to approximate the (unknown) value appropriate for our surface, which was grass about 30 cm tall but thin and sparse. Decreasing  $z_0$  to 2 mm changes the profile considerably, not only by reducing  $L$  through  $u_*$  but also by concentrating more of the gradient near the surface due to the smaller value of eddy diffusivity there. Although neither theoretical profile compares well overall with the experimental data, presumably because of the nonuniform ionization referred to above, the difference in computed ion-density ratios between 1 m and 20 cm agrees fairly well with the same difference in the measured conductivity ratios listed in columns 12 and 13 of Table 2.

The results of this experiment can be summarized as follows. First, although there is some basis for questioning the conductivities measured at 1 m, the relative maximum in  $\lambda_+$  observed at that level is unlikely to have been caused by the lack of equalization of the instrument and is probably real. Second, accepting these data lends support to the theoretical predictions resulting from the supposed diffusion of ions to the absorbing lower boundary. Third, the present data conflict with those published by Higazi and Chalmers [16] in that they show a strong *increase* in both polar conductivities with height in the lowest meter.

## SURFACE-CURRENT EXPERIMENT

I carried out another experiment at the Waldorf site in an effort to test the hypothesis that the current is diffusion rather than conduction at the ground. The concept behind this experiment can be described as follows. Hoppel [6] and I [8] have shown that the boundary condition of vanishing ion density at the surface results in the buildup of a peak in the charge-density profile at the top of a thin diffusion sublayer. This peak is maintained from above by convergence of conduction current and is eroded from below by turbulent diffusion down the gradient to the absorbing lower boundary. If the conduction current could suddenly be shut off at some level above the charge-density maximum, the theories predict that the current at the surface would not stop immediately. Instead it should gradually decay as the space charge is depleted by diffusion to the surface.

Since the total current arriving at the ground by all mechanisms can be measured with a flush-mounted Wilson plate, such as that used by Aspinall [20], it should be possible to test the absorbing boundary condition there by comparing the current received by exposed and electrostatically shielded plates. The exposed plate is used to monitor the total current density. Another

identical plate is covered with a grounded wire mesh to shield it from the ambient electric field while allowing the natural space-charge profile to be advected across it by the wind. If the lower-boundary conditions used by Hoppel and by myself are correct, the covered plate should measure a nonnegligible fraction of the current received by the exposed plate. Furthermore, since the thickness of the diffusion sublayer and the rate at which charge is advected both increase with increasing wind, this fraction should increase with wind speed. If all the current at the surface is carried by conduction, on the other hand, then cutting off the field should result in no current being measured by the covered plate.

The two Wilson plates used in my experiment were 2.44-by-3.05-m (8-by-10-ft) aluminum frames covered with sheet aluminum and set on insulating pads in pits about 0.3 m (1 ft) deep (Fig. 3). All aluminum surfaces were treated with Iridite<sup>TM</sup> dip, a proprietary mixture in which the main ingredient is chromic acid, producing a weather-resistant but electrically conductive finish. In operation, both plates were covered with rough carpet, shown on the front plate in the photograph, to make their surface geometry more similar to that of the surrounding short grass. This carpet was a commercial vinyl material which was sprayed with rubber-based carbon paint to make it electrically conducting.

The electrostatic shield, shown on the front plate in Fig. 3, was made of 0.81-mm-diameter (0.032-in.-diameter) galvanized steel chicken wire with a 51-mm (2-in.) hexagonal mesh. This screen was stretched over the top and sides of a 3.0-by-3.7-m (10-by-12-ft) aluminum frame standing 0.61 m (2 ft) high. The frame could be lowered over one of the current plates so as to completely cover it with screen, leaving a clearance of about 0.3 m (1 ft) all the way around. Measurements and calculations agree that this arrangement was effective at shielding the plate from more than 98% of the ambient field.

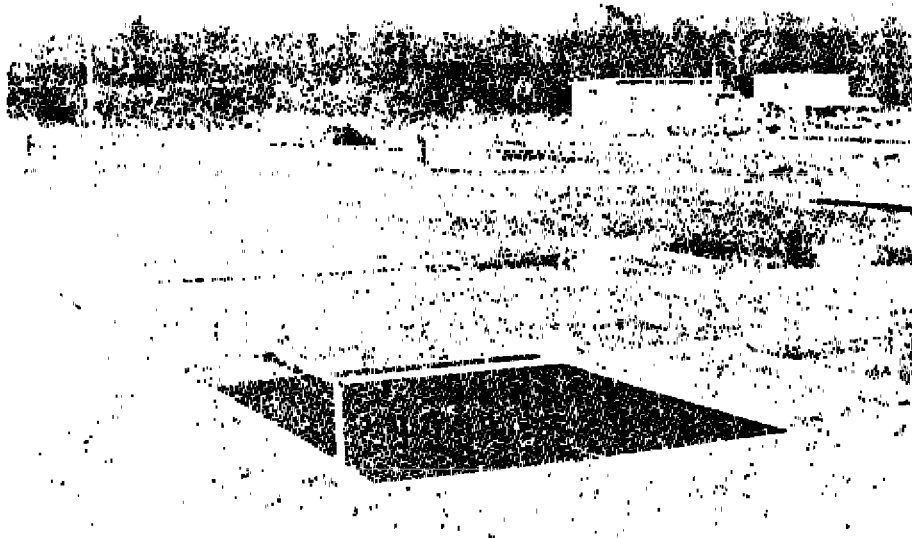


Fig. 3 — Wilson plates used for the surface-current experiment. The near plate is covered with rough carpet (black) and shielded from the external field by a grounded chicken-wire screen. The pits visible downwind (at the right in the photograph) are for additional current plates.

The plates were connected to current amplifiers similar to those used in the Gerdien conductivity tubes described earlier. Thus each plate was held within a few millivolts of ground potential throughout the measurements. In addition the amplifiers were provided with variable polystyrene feedback capacitors so that their time constants could be matched to that of the atmosphere as described by Kasemir [26], if desired. The calibration of the two amplifiers was identical: 1.94 V per pA/m<sup>2</sup> ± 2%, accounting for the geometrical plate areas of 7.29 m<sup>2</sup>. Furthermore, the average currents measured by the two plates, when both were simultaneously exposed, agreed within 1%.

Because the plates were held at ground potential, any contact potential between their undersides and the bottom of the pits must have caused a nonzero electric field there. The resulting error currents flowing through the air between the plates and the soil are not easily distinguished from the residual convection current to be measured. Therefore, tests were carried out to assess their magnitude and behavior.

The situation can be illustrated by the equivalent circuit in Fig. 4. The voltage  $V_o$  is the "open-circuit" voltage of an exposed current plate disconnected from its amplifier. The current  $I_A$ , the fair-weather atmospheric current to the plate, is balanced in the steady state by the leakage current through the resistance  $R$  of the air between the plate and the ground. The battery  $\Delta V$  represents the contact potential between these two conductors. The open-circuit voltage is determined by

$$I_A = (V_o - \Delta V)/R.$$

If the plate is connected to a low-impedance current meter, the short-circuit current  $I_s$  is given by

$$I_s = I_A + \Delta V/R = V_o/R.$$

Thus, the fractional measurement error is

$$\frac{I_s - I_A}{I_s} = \frac{\Delta V}{V_o}.$$

This expression emphasizes the importance, already pointed out by Kasemir and Ruhnke [27], of designing current antennas to have large open-circuit voltages. The  $V_o$  of the Waldorf plates

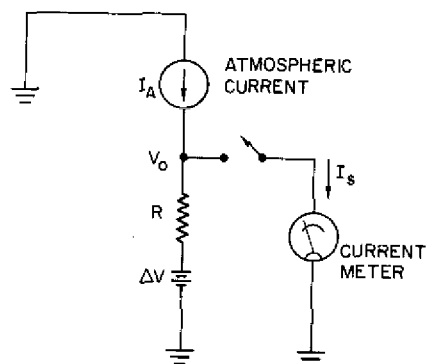


Fig. 4 — Equivalent circuit for a current plate.  $V_o$  and  $I_s$  are respectively the open-circuit voltage (switch open) and short-circuit current (switch closed).  $R$  represents the open-circuit resistance of the plate to ground. The battery  $\Delta V$  represents the contact potential between the plate and ground.

measured only about 4.5 V in a 100-V/m field. Comparison of this voltage with a typical contact potential of -0.3 V (the measured open-circuit voltage of a *covered* plate with several radioactive sources installed in the pit beneath to increase the conductivity there and thus to minimize other effects on the open-circuit voltage) implies a fractional measurement error of 7%.

This error is too large to permit accurate determination of the fair-weather current density, but it should not cause much trouble in the present context, for the following reasons. First, although the contact potential between two conductors of different materials is often as high as 1 V, its change with time and weathering is generally smaller — perhaps only a few tenths of a volt. Second, we will be principally concerned with correlations of the measurements with wind speed, and there is no reason to expect the contact potentials to depend directly on that parameter. Therefore, any errors caused by contact potentials will be ignored in the following.

Before the results of the surface-current experiment are presented, the theory of the turbulent electrode effect must be further articulated so that its predictions are definite. A charge-density profile will be derived here for the diffusion sublayer and will be used to compute the net convection current to a covered plate under various conditions. The starting point for this analysis is the ion-density profile derived in the previous section as Eq. (1). For small enough  $z/L$ , this implies the following approximate conductivity profile:

$$\lambda(z) \approx \lambda_\infty \left[ 1 - \ln(2\sqrt{z/L}) / \ln(2\sqrt{z_0/L}) \right]. \quad (2)$$

In a steady-state, horizontally homogeneous surface layer with eddy diffusivity  $\kappa(z) = Kz$ , as was defined on page 4, the continuity equation integrates to

$$-Kz \frac{d\rho}{dz} + \lambda E = J_0,$$

where  $\rho$  is the space-charge density and  $J_0$  is the (uniform) total current density. Assuming that the electric field remains approximately equal to its surface value throughout this thin layer and using Eq. (2) and the homogeneous lower boundary condition  $\rho(z_0) = 0$ , we can solve this equation and obtain

$$\rho(z) = -\frac{J_0}{K} \ln \frac{z}{z_0} - \frac{\lambda_\infty E_0}{4K \ln(2\sqrt{z_0/L})} \ln^2 \frac{z}{z_0}. \quad (3)$$

Equation (3) represents the charge-density profile in the ambient atmosphere as it enters the upwind side of the screen over the covered current plate.

Beneath the screen the situation is no longer horizontally homogeneous; the charge density decays in the downwind ( $x$ ) direction due to diffusion to the surface. The partial differential equation expressing the two-dimensional charge distribution in this steady-state problem is

$$u \frac{\partial \rho}{\partial x} = K \frac{\partial}{\partial z} z \frac{\partial \rho}{\partial z},$$

where  $u(z)$  is again the wind speed. This relation equates the horizontal convergence of charge due to advection by the mean wind to its vertical divergence by turbulent transport. The following additional terms have been dropped: the horizontal turbulent transport, the vertical mean advection

(subsidence), and the conduction currents due to horizontal and vertical electric fields beneath the screen.

In addition to the initial condition of Eq. (3) at  $x = 0$  and the homogeneous lower-boundary condition, the solution of this partial differential equation requires an upper-boundary condition. For simplicity, we will assume that the peak of the charge-density profile stays at the same height above the surface as the space charge decays, giving the condition  $\partial\rho/\partial z|_{z=z_1} = 0$ . (Actually, the height of the peak should move upward with downwind distance, so this approximation will deplete the space-charge peak too rapidly, resulting in an underestimate of the net current to the covered plate.) The height  $z_1$  of the upper boundary is computed from Eq. (3) as

$$\ln \frac{z_1}{z_0} = \frac{J_0}{\lambda_\infty E_0} \left( \ln \frac{L}{z_0} - 2 \ln 2 \right).$$

Before proceeding, it is convenient to throw the partial differential equation and its initial and boundary conditions into dimensionless form according to the definitions  $\rho \equiv [(-J_0)/K]\rho'$ ,  $z \equiv z_0 z'$ ,  $x \equiv z_0 x'$ ,  $\delta \equiv L/z_0$ , and  $\gamma \equiv J_0/\lambda_\infty E_0$ . This yields

$$\ln z' \frac{\partial \rho'}{\partial x'} = 0.17 \left( z' \frac{\partial^2 \rho'}{\partial z'^2} + \frac{\partial \rho'}{\partial z'} \right), \quad z' \ni [1, z'_1], \quad (4a)$$

$$\ln z'_1 \equiv \gamma(\ln \delta - 2 \ln 2), \quad (4b)$$

$$\left. \frac{\partial \rho'}{\partial z'} \right|_{z'=z'_1} \equiv 0, \quad (4c)$$

$$\rho'(x' = 0) = \ln z' - \frac{1}{2 \ln z'_1} \ln^2 z', \quad (4d)$$

and

$$\rho'(z' = 0) \equiv 0, \quad (4e)$$

where we have used the logarithmic wind profile  $u(z) = (u_*/0.35) \ln(z/z_0)$  and  $K = 0.47u_*$ , as before. The surface-current density is then given by  $J(z'_0, x') = J_0 \partial \rho' / \partial z' |_{z'=1}$ .

The system of equations (4) has been solved numerically by the implicit method of Crank and Nicholson, cited by Richtmyer and Morton [28], after logarithmic stretching of the vertical coordinate to allow sufficient resolution near the lower boundary. By taking  $\gamma = 0.5$ , in acknowledgment of the theoretical result that the surface field should be about twice the field above the convection-current layer, solutions have been calculated for two values of  $\delta$ . A wind of 4 m/s over a surface with roughness length  $z_0 = 2$  mm (second row of Table 3) implies  $\delta = 1250$ ; cutting the wind speed in half reduces  $\delta$  to 625. Figure 5 shows the dimensionless surface-current density  $J(z'_0, x')/J_0$  as a function of normalized horizontal distance  $x/z_0$  from the upwind edge of the screen for the two cases.

Table 4 summarizes the values of various numerical results, including the height  $z_1$  and magnitude  $\rho_{\max}$  of the initial charge-density peak. Column 6 gives the integrated charge per unit horizontal

area  $\sigma$  between the surface and this peak, allowing an estimate of the electric-field perturbation in the diffusion sublayer. Column 7 gives the integrated current per unit width advected through the upwind side of the screen between the surface and the peak. Finally, the last column gives the predicted ratio of the net currents measured by the covered and exposed plates, assuming that the former extends from  $x' = 152$  to 1372 ( $x = 0.30$  to 2.74 m) as shown in Fig. 5.

We now can justify a posteriori some of the assumptions. Consider the  $\delta = 1250$  case and suppose  $J_0 = -0.5$  pA/m<sup>2</sup> (a typical value observed during this experiment). This implies the following dimensional results:  $z_1 = 3.5$  cm,  $\rho_{\max} = 8.5$  pC/m<sup>3</sup>,  $\sigma = 0.24$  pC/m<sup>2</sup>, and  $j = 0.27$  pA/m. First, it is easily verified that  $z_1/L = 0.014$  is small enough for Eq. (2) to be a good approximation to the conductivity profile. Second, the change in electric-field strength through the diffusion sublayer, given by  $\sigma/\epsilon_0 = 0.028$  V/m, is indeed negligible. Third, even if we use the maximum charge density throughout the entire volume beneath the screen, the maximum fields there are only of the order of  $\rho_{\max} h/2\epsilon_0 = 0.29$  V/m, where  $h = 0.61$  m is the height of the screen above the plate. Thus it is reasonable to ignore conduction beneath the screen. Finally, as confirmation of the accuracy of the partial-differential-equation solution leading to Fig. 5, the current  $j$  advected under the screen exactly equals the integral over  $x$  of the surface-current density  $J(z_0, x)$  in each case.

Now we can discuss the measurements made during June and July 1979. Polar conductivities and charge density at the 20-cm level and wind speed and direction at 5 m were recorded during data runs as described earlier for the conductivity-profile experiment. Additional data were recorded from the two current plates and a five-anemometer wind-profile system as will be described. All runs were in daytime with sky conditions ranging from clear to broken fair-weather cumuli. The data are presented in Table 5.

Except for run 10 and brief comparison checks at the beginning of each day, the current plates were always operated with one covered and the other exposed, as shown in Fig. 3. The amplifier for the covered plate was given a time constant of 108 s (0.004  $\mu$ F in parallel with the 27-G $\Omega$ \* feedback resistor) to smooth the trace sufficiently for easy averaging. An attempt was made to keep the exposed plate close to Kasemir's phase-matched condition in order to reduce its sensitivity to displacement-current fluctuations. Each morning its feedback capacitance was adjusted to give the best square-wave response to step changes in an artificially applied field. This resulted in a time constant of 1890 s (0.07  $\mu$ F) on all days except June 14, when the time constant was 2430 s (0.09  $\mu$ F).

To measure the surface-roughness length and to get a better estimate of the friction velocity than was available from the wind speed at 5 m alone, a wind profiling system was operated during this experiment. It consisted of five sensitive cup anemometers (Thorntwaite Associates model 912, with a starting speed <8.9 cm/s and a distance constant of 83 cm) mounted on a pole at heights of 18, 36, 53, 89, and 160 cm (7, 14, 21, 35, and 63 in.) above the ground, as shown in Fig. 6. The associated electronics, housed in the small white box visible in the foreground, accumulated the pulses from each anemometer and relayed voltages proportional to the integrated wind run to the data system for recording. For the five data runs on June 14 and 15 the anemometer at 36 cm was not operating, but for the others data were obtained from all five instruments.

These wind data were analyzed as follows. With use of a nonlinear, least-squares, curve-fitting algorithm, the formula

$$u(z) = \frac{u_*}{k} \left[ \ln \left( \frac{z-d}{z_0} \right) - \psi(\phi) \right],$$

\*1 G $\Omega = 10^9 \Omega$ .

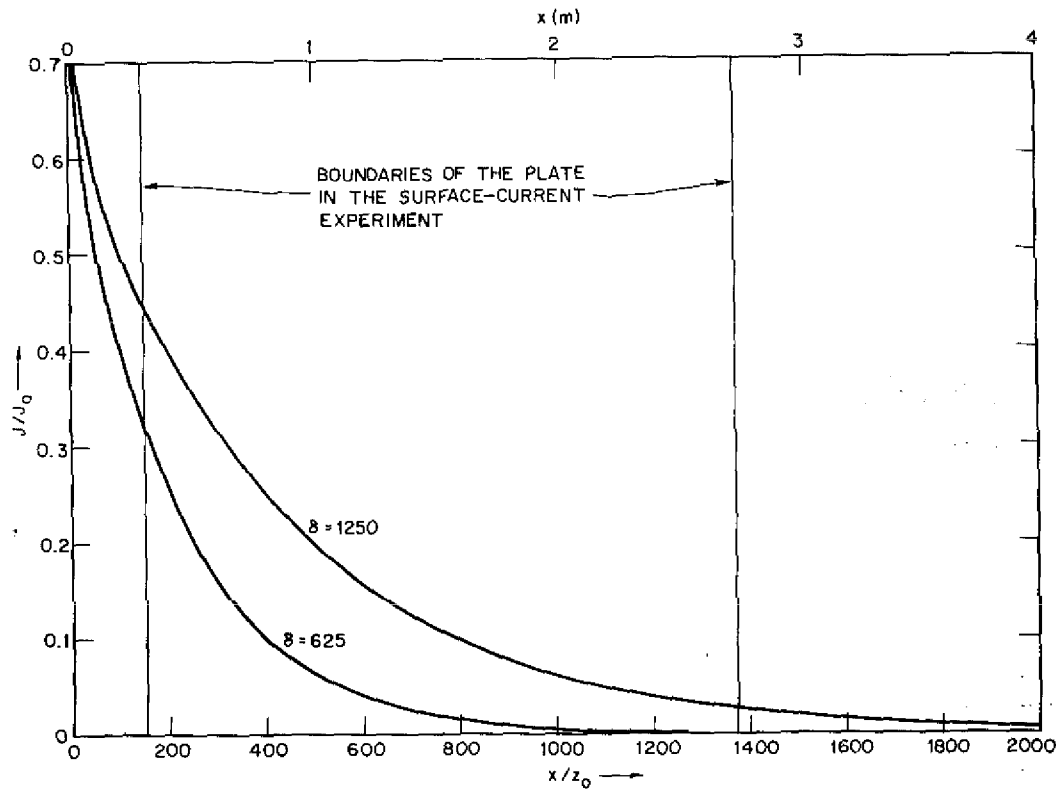


Fig. 5 — Theoretical distribution of normalized current density across the covered plate. The horizontal distance  $x$  is measured from the upwind edge of the idealized electrostatic shield in units of roughness length. With the assumption that  $z_0 = 2$  mm, the upper scale shows this dimension in meters. For  $\gamma \equiv J_0/\lambda_\infty E_0 = 0.5$  two curves are shown for different values of  $\delta \equiv L/z_0$ , as in Table 4.

Table 4 — Results of the approximate calculation of net current to the covered plate for  $z_0 = 2$  mm,  $\gamma \equiv J_0/\lambda_\infty E_0 = 0.5$ , and two wind speeds. The last column gives the predicted ratios of the net currents measured by the covered and the exposed plates.

$u$ (5m) (m/s)	$K$ (m/s)	$\delta$ $\equiv L/z_0$	$z'_1$ $\equiv z_1/z_0$	$\rho'_{max}$ $\equiv \rho_{max} K/(-J_0)$	$\frac{\sigma K}{z_0(-J_0)}$	$\frac{j}{z_0(-J_0)}$	Net- Current Ratio (%)
4	0.085	1250	17.7	1.44	20.6	274	14.7
2	0.042	625	12.5	1.26	12.2	140	5.6

Table 5 — Average data for each run in the 1979 surface-current experiment. Data are omitted for runs 1 to 4 because the wind direction, although acceptable for the current plates, yielded too short a fetch for the conductivity, space-charge, and wind-profile instrumentation.

Run	Date (1979)	Length (min)	Wind Speed (m/s)	Polar Conductivity ( $10^{-14}$ mho/m)		Space Charge ( $\text{pC/m}^3$ )	$u_*/k$ (cm/s)		Current to Plates ( $\text{pA/m}^2$ )		Current Ratio (%)	Field* (V/m)
				$\lambda.2A$	$\lambda.2B$		Neutral	$L^*$ = -10 m	Covered	Exposed		
1	July 2	15	4.11	—	—	—	—	—	-0.036	-0.39	9.3	—
2	July 2	25½	3.84	—	—	—	—	—	-0.041	-0.37	11	—
3	July 2	42	3.20	—	—	—	—	—	-0.026	-0.36	7.1	—
4	July 2	28½	3.06	—	—	—	—	—	-0.067	-0.57	12	—
5	June 22	15	2.68	0.772	-0.645	7.2	42	54	-0.021	-0.64	3.2	-45
6	July 9	20	2.44	0.697	-0.609	8.9	28	36	-0.026	-0.57	4.5	-44
7	June 14	15	2.43	0.347	-0.331	6.2	36	47	-0.013	-0.49	2.6	-72
8	July 9	15	2.38	-0.618	0.634	8.9	30	39	-0.010	-0.62	1.7	-50
9	June 14	20	2.24	-0.314	0.313	6.3	34	43	0.008	-0.48	-1.6	-77
10	June 15	40	2.01	0.648	-0.581	11.9	31	40	-0.66 †	-0.66	—	-54
11	July 9	25	1.96	0.663	-0.597	8.3	25	33	-0.005	-0.57	0.9	-45
12	June 22	10	1.92	0.825	-0.272 <sup>‡</sup>	8.8	29	38	-0.010	-0.64	1.6	—
13	June 14	30	1.85	-0.418	0.414	8.4	28	37	-0.018	-0.54	3.3	-65
14	June 27	10	1.58	0.978	-0.817	11.7	20	26	-0.052	-0.80	6.5	-45
15	June 14	10	1.44	0.445	-0.396	9.1	23	30	-0.003	-0.63	0.4	-75
16	June 27	10	1.33 <sup>‡</sup>	-0.811	0.931	17.5	29 <sup>‡</sup>	37	-0.062	-0.98	6.3	-56

\*"Field" is calculated by dividing the current to the unexposed plate by the total measured conductivity.

where

$$\psi(\phi) \equiv \ln \left[ \frac{(1 + \phi)^2 (1 + \phi^2)}{8} \right] - 2 \tan^{-1} \phi + \pi/2$$

and

$$\phi(z) \equiv \left[ 1 - 15 \left( \frac{z - d}{L_*} \right) \right]^{1/4},$$

was fitted to all 12 runs for which reliable wind data were available. This was done in such a way that each run determined its own value of  $u_*/k$  but  $z_0$  and  $d$  (zero-plane displacement) were forced to be the same for all runs. The Obukhov length  $L_*$ , the only other parameter in this formulation taken from Businger [29], was unknown because no temperature information was available. It was assumed that  $L_* \rightarrow \infty$  (neutral stability) so that  $\phi \equiv 1$ ,  $\psi \equiv 0$ , and  $u(z)$  reduced to the well-known logarithmic wind profile. This yielded  $z_0 = 2.0$  mm,  $d = 6.0$  cm, and the values of  $u_*/k$  shown in column 8 of Table 5. Then, to assess the effect of departures from neutrality,  $L_*$  was set to  $-10$  m, appropriate for moderately strong instability. The results became  $z_0 = 6.6$  mm,  $d = 1.9$  cm, and the values of  $u_*/k$  in column 9 of the table, which are seen to be about 30% larger than those in the previous column.

In addition to determining  $z_0$ , the wind-profile measurements represented the only convenient way of testing our mixing-length assumption that the eddy-diffusion coefficient could be expressed as  $\kappa(z) = Kz$ . Since this form leads to the logarithmic wind profile, the ability to fit the data accurately with such a profile would lend credibility to that assumption. Figure 7 shows the results under the neutral assumption for a representative selection of runs. The fit is quite good except for some

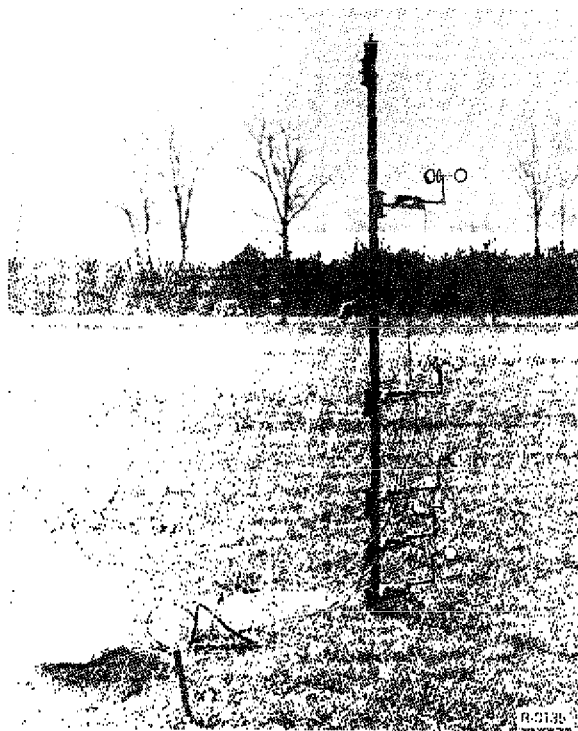


Fig. 6 — System for measuring wind profiles. Five cup anemometers are shown at heights of 18, 36, 53, 89, and 160 cm above the ground. The white box downwind (foreground in the photo) contains the associated electronics.

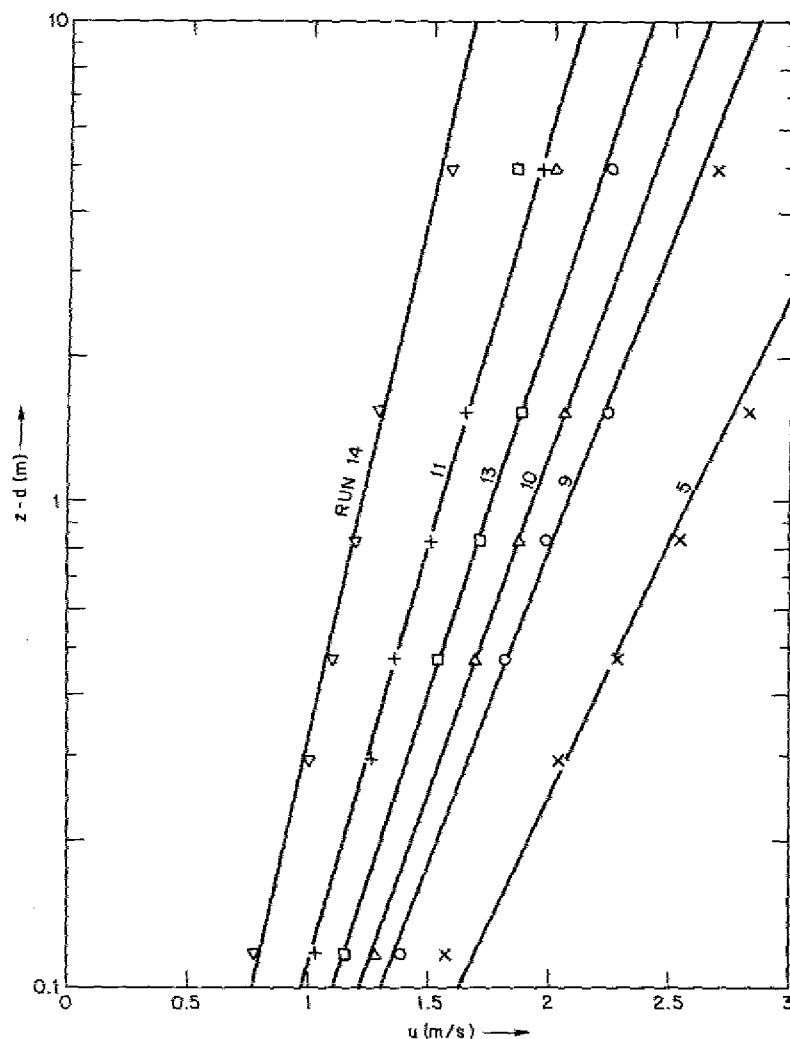


Fig. 7 — Wind profiles for a representative selection of runs. For each run, all data points are plotted with a common symbol, and the corresponding least-squares fit is labeled with the run number, as given in Table 5. The uppermost row of plotted points indicates the mean wind speeds at 5 m, which were not used in fitting the profiles and have been shown for comparison only.

of the points at 5 m, which were taken with a different kind of instrument on a tower separated horizontally by about 20 m from the profile instrumentation. The overall RMS deviation of the profile measurements (55 mean wind-speed values) from the logarithmic curves (14 free parameters) is only 0.067 m/s.

In spite of the relatively poor agreement of the 5-m wind speeds with the extrapolated profiles, the correlation between  $u(5\text{ m})$  and  $u_* / k$  (columns 4 and 8 in Table 5) is good. Discarding the obvious outlier, run 16, where  $u(5\text{ m})$  is less than the profile winds at all but the 18-cm level, we find a correlation coefficient of 0.84! The corresponding linear regression line implies  $z_0 = 2.8\text{ mm}$ , in acceptable agreement with the profile measurements. Because of the lack of profile-derived values of  $u_* / k$  in the four runs of highest wind speed, the 5-m wind will therefore be used in place of the friction velocity in the following. Run 16 will be omitted from further consideration.

20. Abstract (Continued)

measurement of the nonconductive component of the vertical current density at the ground, tends to confirm a crucial assumption of the theories that all of the current is carried by turbulent and molecular diffusion at the surface. Suggestions are given for further experimental and theoretical work.

All of this suggests, without proving, that the eddy-diffusion formulation leading to Eqs. (1) and (4) is reasonable and that the fetch was probably sufficient for the surface layer to be in equilibrium throughout the lowest meter or so. Since the ion-density profiles are presumably dominated by turbulent transport in this region, they should also be in equilibrium. The charge-density maximum is controlled by the conduction current; but since the total charge per unit area in the lowest meter is small enough to be replenished by the total current density in only 10 to 20 s, it should be in equilibrium too. This justifies a comparison of the data in Table 5 to the theoretical predictions in Table 4.

The ratios of the current measured by the covered and uncovered plates are listed in the second-last column of Table 5. The correlation coefficient of these ratios with the 5-m wind speed (excluding runs 10 and 16) is 0.72, significantly different from zero at the 1% level. Furthermore, the corresponding linear regression line yields values of 10% at 4 m/s and 2.6% at 2 m/s, which is a fairly good match with the theoretical estimates in the last column of Table 4. It remains to consider other mechanisms which might produce this apparent agreement.

Several physical processes, in addition to the turbulent diffusion of space charge, could cause the covered plate to measure a significant fraction of the total current density. One process, already mentioned, is the conduction current beneath the plate due to a contact potential between the metal and the soil. Although this mechanism cannot be ruled out in the present context, its effects are discounted here because it should not display the observed wind-speed dependence. In fact, one might speculate that the conductivity of the air under a current plate should decrease with increasing wind, due to the flushing of trapped radon gas, leading to a decrease in this error current with increasing wind speed.

Two other sources of current to the covered plate become available if we assume that the theory is wrong and that the current is really carried by conduction at the surface. First, the leakage of the external field through the grounded screen, which was stated earlier to be less than 2%, would contribute the same fraction to our ratio. Second, the space charge beneath the screen produces its own electric field at the plate, through Gauss's law. Measured charge densities in column 7 of Table 5 agree well with the values calculated from Table 4 and are too small to cause trouble. Furthermore, both the ambient field and the space charge seem to show the wrong dependence on wind speed. The field was not measured directly in this experiment, but a crude estimate based on the total conductivity and the current to the exposed plate is shown in the last column of Table 5. Both the magnitude of this "field" and the charge density show negative correlations with wind speed, although they are not statistically significant. Referring back to the conductivity-profile experiment, we again find negative correlations with wind speed for both pole-top potential and charge density as well as a strong correlation (0.77) between these two parameters which is significant at the 1% level.

The results of this experiment can be summarized as follows. There appears to be a significant increase with wind speed in the fraction of the total current density collected by an electrostatically shielded, roughly surfaced Wilson plate. This observation apparently cannot be explained away by any known physical process. It is therefore taken as evidence in support of the hypothesis that the current is transferred by turbulent diffusion, rather than by conduction, at an aerodynamically rough surface under conditions of strong mixing.

## SUMMARY AND CONCLUSIONS

The theory of the turbulent electrode effect, as developed by Hoppel [6] and extended by me [8], requires that both polar conductivities decrease toward the ground and that the fair-weather

current be carried by diffusion at the surface under conditions of strong turbulent mixing. I have here further articulated this theory to yield definite predictions about the conductivity profiles and the behavior of the surface-current density over a field of grass. These predictions have been tested by two experiments designed to identify the effects of the hypothesized turbulent diffusion of ions and space charge to the absorbing lower boundary.

The results of the experiments, described in the preceding sections, support the theoretical predictions. The conductivity-profile experiment gives evidence that both polar conductivities do indeed decrease toward the ground, at least over the lowest meter. This is a direct contradiction of the previous results of Higazi and Chalmers [16]. The present results, however, confirm the observations of those authors that the ratio of negative to positive conductivity near the surface increases toward unity with increasing wind speed. The surface-current experiment gives evidence that at least part of the current at the surface is carried by turbulent diffusion. The observed fraction of the fair-weather current received by the electrostatically shielded plate has roughly the predicted magnitude and shows the correct dependence on wind speed.

These results show that the existing theory of the turbulent electrode effect is at least qualitatively correct. In particular the experimental evidence supports the hypothesis of an absorbing lower boundary and the conclusion that the classical electrode effect gives way to turbulent diffusion of ions to the surface. If true, this has significant implications for the modeling of convection currents in the planetary boundary layer, as I pointed out previously [2]. It means that only the charge-conservation equation need be modeled, with the electrode-effect charge source provided by conduction in the presence of an externally specified conductivity profile. This greatly simplifies the solution from that attempted by Hoppel and Gatham [7], who used conservation equations for each of four species of ions.

Unfortunately, several flaws in the present experiments make their results less dramatic than desired. Future attempts to measure conductivity profiles in the lowest 5 meters should be performed at a site with a longer and more uniform upwind fetch and should take pains to equalize the instruments at *all* levels to the ambient potential. The surface-current experiment should also be repeated using current plates covered with natural sod, to more closely match the roughness of the surrounding surface, and designed to reduce the contact-potential error. The signal-to-noise ratio of this experiment should also be improved by making the plates narrower in the wind direction so as to catch a larger fraction of the diffusion current (the theoretical result of this change being implied by Fig. 5). These improvements should allow a more quantitative test of the theory and more compelling results.

One aspect of my [8] theory that should receive more attention is the treatment of the aerodynamically rough surface. By assuming that the homogeneous boundary conditions for ion density and space charge should be applied at the roughness height, I have probably exaggerated the flux of these quantities to the ground. A repetition of the experiments described in this report, with the modifications suggested, should allow the degree of this overestimate to be assessed.

## ACKNOWLEDGMENTS

I thank R. V. Anderson for his considerable help in setting up the experiments and for many useful suggestions during the preparation of this document. Acknowledgment is also due to W. A. Hoppel for his reading and constructive criticism of the manuscript.

## REFERENCES

1. J. A. Chalmers, *Atmospheric Electricity*, second edition, Pergamon, Oxford, 1967.
2. J. C. Willett, "Fair weather electric charge transfer by convection in an unstable planetary boundary layer," *J. Geophys. Res.* **84**, 703-718 (1979).
3. W. A. Hoppel, "Theory of the electrode effect," *J. Atmos. Terr. Phys.* **29**, 709-721 (1967).
4. F. J. W. Whipple, "On potential gradient and the air earth current," *Terr. Magn. Atmos. Elect.* **37**, 355-359 (1932).
5. P. N. Tverskoi and M. P. Timofeev, "Turbulence and the vertical profile of electric field intensity in the lower layer of the atmosphere," *Izvestiia Akademii Nauk SSSR, Seriiia geograficheskaiia i geofizicheskaiia* **12**, 377-386 (1948).
6. W. A. Hoppel, "Electrode effect: comparison of theory and measurement," pp. 167-181 in *Planetary Electrodynamics*, Vol. II, S. C. Coroniti and J. Hughes, editors, Gordon and Breach Science Publishers, New York, 1969.
7. W. A. Hoppel and S. G. Gathman, "Determination of eddy diffusion coefficients from atmospheric electrical measurements," *J. Geophys. Res.* **76**, 1467-1477 (1971).
8. J. C. Willett, "An analysis of the electrode effect in the limit of strong turbulent mixing," *J. Geophys. Res.* **83**, 402-408 (1978).
9. R. Muhleisen, "Electrode effect measurements above the sea," *J. Atmos. Terr. Phys.* **20**, 79-81 (1961).
10. P. Pluvinage and P. Stahl, "La conductibilité électrique de l'air sur l'inlandsis Groenlandais," *Annal. de Géophys.* **9**, 34-43 (1953).
11. L. H. Ruhnke, "Electrical conductivity of air on the Greenland ice cap," *J. Geophys. Res.* **67**, 2767-2772 (1962).
12. W. D. Crozier, "Electrode effect during nighttime low-wind periods," *J. Geophys. Res.* **68**, 3451-3458 (1963).
13. W. D. Crozier, "Atmospheric electrical profiles below three meters," *J. Geophys. Res.* **70**, 2785-2792 (1965).
14. W. D. Crozier and N. Biles, "Measurements of radon 220 (thoron) in the atmosphere below 50 centimeters," *J. Geophys. Res.* **71**, 4735-4741 (1966).
15. A. R. Hogg, "The conduction of electricity in the lowest levels of the atmosphere," *Memoirs of the Commonwealth Solar Observatory*, Canberra, No. 7, 1939.
16. K. A. Kigazi and J. A. Chalmers, "Measurements of atmospheric electrical conductivity near the ground," *J. Atmos. Terr. Phys.* **28**, 327-330 (1966).
17. W. A. Hoppel and S. G. Gathman, "Experimental determination of the eddy diffusion coefficient over the open ocean from atmospheric electric measurements," *J. Phys. Oceano.* **2**, 248-254 (1972).
18. C. J. Adkins, "The small-ion concentration and space charge near the ground," *Q. J. Roy Met. Soc.* **85**, 237-252 (1959).
19. J. Law, "The ionisation of the atmosphere near the ground in fair weather," *Q. J. Roy Met. Soc.* **89**, 107-121 (1963).
20. W. P. Aspinall, "Mechanical-transfer currents of atmospheric electricity," *J. Geophys. Res.* **77**, 3196-3203 (1972).

WILLETT

21. S. G. Gatham and E. M. Trent, "Absolute Electric Field Measurements Using Field Mills," NRL Report 6538, Apr. 1967.
22. R. V. Anderson and H. Dolezalek, "Atmospheric electricity measurements at Waldorf, Maryland during the 7 March 1970 solar eclipse," *J. Atmos. Terr. Phys.* **34**, 561-566 (1972).
23. S. Gatham, "Guarded double field meter," *Rev. Sci. Inst.* **39**, 43-47 (1968).
24. S. G. Gatham and E. M. Trent, "Atmospheric Potential-Gradient Measurements at Sea," NRL Report 7030, Feb. 1970.
25. R. V. Anderson, "Absolute measurements of atmospheric charge density," *J. Geophys. Res.* **71**, 5809-5814 (1966).
26. H. W. Kasemir, "Measurement of the air-earth current density," pp. 91-95 in *Proceedings on the Conference on Atmospheric Electricity*, R. E. Holzer and W. E. Smith, editors, Geophysical Research Papers 42, Air Force Cambridge Research Center, Bedford, Mass. 1955.
27. H. W. Kasemir and L. H. Ruhnke, "Antenna problems of measurement of the air-earth current", pp. 137-147 in *Recent Advances in Atmospheric Electricity*, L. G. Smith, editor, Pergamon, New York, 1958.
28. R. D. Richtmyer and K. W. Morton, *Difference Methods for Initial-Value Problems*, second edition, Interscience, New York, 1967.
29. J. A. Businger, "Turbulent transfer in the Atmospheric Surface Layer," pp. 67-100 in *Workshop on Micrometeorology*, D. A. Haugen, editor, American Meteorological Society, Boston, 1973.

## CONTENTS

INTRODUCTION .....	1
THEORETICAL BACKGROUND .....	2
PREVIOUS EXPERIMENTAL WORKS .....	4
CONDUCTIVITY-PROFILE EXPERIMENT .....	8
SURFACE-CURRENT EXPERIMENT .....	15
SUMMARY AND CONCLUSIONS .....	25
ACKNOWLEDGMENTS .....	26
REFERENCES .....	27



## TOWARD AN UNDERSTANDING OF THE TURBULENT ELECTRODE EFFECT OVER LAND

### INTRODUCTION

Of all the problems of fair-weather atmospheric electricity, the "electrode effect" has been one of the most studied and most puzzling. According to Chalmers [1], the electrode effect is defined as the nonuniformity of electrical conditions close to an electrode, with the electrode of interest in atmospheric electricity usually being the earth's surface. This definition is rather broad, however. When most investigators use the term, they have in mind only those inhomogeneities caused by the drift of atmospheric ions in response to an electric field normal to the electrode. For example, in a motionless, aerosol-free atmosphere of uniform ionization, the fair-weather electric field sweeps negative ions away from the surface. This results in a layer of positive space charge through which, toward the ground, the field magnitude increases and the total conductivity decreases by roughly a factor of 2. This simple phenomenon will be referred to here as the "classical" electrode effect.

Unfortunately, the situation in the real atmosphere is in general greatly complicated by aerosol particles, nonuniform ionization, and turbulence. In response to these diverse influences the electrode effect assumes various manifestations which can differ drastically from its classical form. Increased ionization rate at the surface can eliminate or reverse the sign of the net space charge. Turbulence can thicken the layer until it is almost undetectable from the surface. This complexity has resulted in much disagreement among experimental results and some confusion about the nature of the electrical processes in the atmospheric surface layer.

In the face of this complexity and confusion, especially after concerted attack by so many researchers over so long a period, it is tempting to dismiss the electrode effect as one of those peculiar little fair-weather problems not deserving further effort. However, this collection of phenomena has considerable implications in other areas of atmospheric electricity. For example, the correct measurement from the ground of parameters of such general importance as the total vertical current density is impossible without understanding the complicating influences of the electrode effect. Even more significant is the fact that the principal surface source of electric charge for convection currents, which have been shown to extend throughout the fair-weather planetary boundary layer, is the electrode effect. I have argued [2] that this process represents a "local generator" which may develop up to 130 kV on occasion.

In recent years Hoppel's work (presented in Ref. 3 and subsequent references cited in this report) and my own work (summarized below) have suggested that strong turbulence, perhaps augmented by the presence of aerosol particles, may cause the electrode effect to separate into two overlapping layers, each controlled by its own set of physical processes. As turbulent transport increases in importance relative to drift in the electric field, the ion-density profiles become dominated by turbulent diffusion, ionization, and recombination or aerosol attachment. This results in a layer (which I shall continue to call the electrode layer, although the classical electrode effect has disappeared entirely) in which the profiles of positive and negative polar conductivity are similar and both decrease toward the surface, where ions are annihilated by attachment or

neutralization. The thickness of this "electrode layer" is controlled by the small-ion lifetime and the turbulence.

The second layer might be called the convection-current layer. The fair-weather electric field tends to build up positive space charge in the electrode layer due to the gradient of conductivity there. In the absence of mixing, this would result in the electric field's increasing toward the surface, so that the conduction-current density could be uniform. The strong turbulence that I hypothesize here, however, rapidly mixes this space charge upward, resulting in a convection-current layer whose thickness is controlled by the electrical relaxation time and the turbulence. In the presence of aerosol particles the relaxation time can be much longer than the ion lifetime, making this layer substantially thicker than the electrode layer. Although the electric field strength may still decrease by about a factor of 2 from the surface to the top of the convection-current layer, little of this decrease and the associated space charge may occur in the electrode layer or be observable from the surface.

In this report I will focus on the preceding model of the turbulent electrode effect. After I review the theoretical background in more detail and summarize the past observations, I will describe two recent experiments to test this new concept of the turbulent electrode effect. My review of the electrode-effect literature is not exhaustive; instead I have tried to cover all of the work relevant to the aspect of the problem at hand, namely, the transformation of the electrode effect in the case of strong turbulent mixing.

## THEORETICAL BACKGROUND

A brief summary of past theoretical work on the nonturbulent electrode effect will serve as an introduction to the turbulent theory. This past work, both with and without aerosol particles and nonuniform ionization profiles, is fully developed and has been thoroughly discussed by Hoppel [3]. The results may be separated into three cases: classical, with aerosols, and with surface radioactivity.

In the so-called classical electrode effect, with uniform ionization rate and no aerosol, the electric-field magnitude decreases to about 45% of its surface value in a layer with a depth of some 2 m (the height required to execute 90% of this decrease if ionization  $q = 10^7 \text{ m}^{-3} \text{ s}^{-1}$ , surface field magnitude  $E_0 = 100 \text{ V/m}$ , recombination coefficient  $\alpha = 1.6 \times 10^{-12} \text{ m}^3 \text{ s}^{-1}$ , and both small-ion mobilities  $k = 1.2 \times 10^{-4} \text{ m}^2 \text{ v}^{-1} \text{ s}^{-1}$ ). This decrease is effected by positive space charge reaching a maximum density of about 370 pC/m<sup>3</sup> (2300 e/cm<sup>3</sup>) at the surface, due to the repulsion of negative ions by the negative (downward) electric field. (The sign convention that vectors are reckoned positive upward will be used throughout this report. Hence in fair weather the field and current density are negative and the potential gradient is positive.) Thus the total conductivity increases with height by about a factor of 2 in the same region. The thickness of this classical electrode layer scales with  $L_c \equiv kE_\infty/(q\alpha)^{1/2}$ , where  $E_\infty$  is the asymptotic magnitude of the field in the interior (as height  $z \rightarrow \infty$ ). Since the mean ion lifetime in the interior is  $\tau_n = (q\alpha)^{-1/2}$ ,  $L_c$  is the distance an ion can drift in the field during its lifetime.

Unfortunately the classical electrode effect is almost never observed, due first of all to the action of aerosol particles as recombination sites for small ions. In consideration of this second case of the nonturbulent theory, Hoppel has shown that when the nucleus count  $Z$  becomes as large as  $10^9 \text{ m}^{-3}$ , the aerosol begins to reduce the small-ion densities and to carry a significant fraction of the space charge. For  $Z \gtrsim 10^{10} \text{ m}^{-3}$ , the small-ion space charge is negligible, and the thickness of the electrode layer is reduced in proportion to the shorter small-ion lifetimes. The

overall decrease in field magnitude with height, however, remains nearly the same, due to higher space-charge density in the thinner layer. This analysis breaks down for  $Z > 10^{11} \text{ m}^{-3}$ , when the electrical mobility of the large ions must be considered.

The third nonturbulent case introduces the effects of trapped radon gas and surface radioactivity. Hoppel has shown that the resulting rapid increase in ionization rate with decreasing height can actually reverse the electrode effect, giving  $E_\infty > E_0$ . There is still a thin layer of positive space charge at the surface, as in the classical electrode effect, but this can be overlain by a thicker layer containing a larger net negative charge, due to the upward drift of negative ions out of the region of high ionization. In the presence of significant aerosol density the effect of surface radioactivity (especially  $\alpha$  emission, which has a range of about 3 cm in air) is considerably increased due to the decrease in layer thickness.

Today it is generally accepted that the principal phenomenon obscuring the electrode effect in observations at the ground is neither the action of aerosol particles nor the effects of trapped radon gas and surface radioactivity but rather convective mixing of space charge in the normally turbulent atmosphere. The first mathematical model of this convection current appears to have been that of Whipple [4]. Assuming uniform total conductivity  $\lambda$  and eddy-diffusion coefficient  $\kappa$ , he showed that in a steady-state, horizontally homogeneous atmosphere charge density supplied at the surface could be carried to heights of the order of 100 m. The height scale of this turbulent "electrode layer" was found to be  $L_T \equiv (\epsilon_0 \kappa / \lambda)^{1/2} \gg L_c$  ( $\epsilon_0 \equiv 8.85 \text{ pF/m}$  being the dielectric permittivity of air), and within the layer the convection current was shown to be opposite in direction and comparable in magnitude to the total fair-weather current. This resulted in an increased downward conduction current and electric field throughout the layer, effectively thickening the electrode effect enough to make it undetectable at the surface.

This model was extended by a number of investigators, such as Tverskoi and Timofeev [5], who used eddy diffusivity increasing linearly with height, without removing the model's basic problem. By assuming a space-charge density at the lower boundary, the investigators sidestep the question of how this charge is produced and in what quantity. The first successful resolution of this difficulty was achieved by Hoppel [6], who constructed a self-consistent model of the turbulent electrode effect over an aerodynamically smooth surface, using the correct lower boundary conditions of vanishing small-ion density. This model was extended by Hoppel and Gathman [7] to include the atmospheric aerosol.

The conclusions from Hoppel's model solutions are briefly as follows. In a thin "diffusion sublayer" at the surface, the positive-small-ion density and conduction current decrease to zero, so that the total downward current is carried by diffusion at the lower boundary. Above this layer, the convection current is upward, carrying the electrode-effect positive space charge into the interior as described by Whipple [4]. Increasing the strength of the turbulence thickens the layer roughly as  $L_T$  but does not change the overall decrease of field magnitude, which remains about a factor of 2. The addition of aerosol particles to the turbulent electrode effect increases the layer thickness by lengthening the electrical relaxation time (which is  $\tau_\lambda = \epsilon_0 / \lambda$  and which appears in the expression for  $L_T$ ), in contrast to its effect in the nonturbulent case. Finally, Hoppel [6] showed that turbulent mixing, in addition to preventing the trapping of radon gas near the surface, also dramatically reduces the effect of increased ionization by vertically mixing the space charge.

In all of Hoppel's solutions for turbulence with uniform ionization, both the negative and the positive small-ion densities decrease toward the surface. This is a result of turbulent and molecular diffusion to the absorbing lower boundary and implies that the total conductivity should increase with height in the electrode layer. The effect becomes more pronounced as the turbulence intensity

increases and was the motivation for my analysis [8] of the electrode layer over an aerodynamically rough surface.

My calculations [8] suggest that, in a limit of strong turbulence that appears applicable in many cases over land, the positive and negative ion-density profiles become similar and decrease toward zero at the ground over a "recombination" layer whose thickness scales with  $L_R \equiv K/(q\alpha)^{1/2} = K\tau_n$ , where the eddy diffusivity has been taken as  $\kappa(z) \equiv Kz$ , with  $K$  being a constant. This means that the total-conductivity profile becomes independent of the electric field and current density in this limit and that the classical electrode effect of separation of ions by conduction at a rigid surface is replaced by turbulent diffusion of ions to an absorbing boundary.

Two predictions of my model are readily testable by field experiments. The first such prediction is that the ratio of positive to negative polar conductivity  $\lambda_+/\lambda_-$  near the surface should decrease toward unity with increasing wind speed and that, under turbulent conditions, the conductivities should both increase with height over a layer whose thickness is roughly proportional to wind speed. The second testable prediction is that, because the total conductivity must vanish at the physical surface, all the current there must be carried by turbulent and molecular diffusion of space charge down its density gradient.

## PREVIOUS EXPERIMENTAL WORKS

The classical electrode effect has been observed on few occasions. Muhleisen [9] reported electric-field profiles over Lake Constance, during very light winds and strong stability in what must have been very clean air, which agree well with calculations.

Pluvinage and Stahl [10] measured the positive and negative polar conductivities simultaneously 1.5 m above the Greenland ice cap, where they found typical values of electric field and nucleus count to be 100 V/m and  $5 \times 10^8 \text{ m}^{-3}$  respectively. Their only low-wind observation (1 m/s) gives  $\lambda_+ = 1.60 \times 10^{-14}$ ,  $\lambda_- = 0.16 \times 10^{-14}$ , and  $\lambda_+ - \lambda_- = 1.64 \times 10^{-14} \text{ mho/m}$ , the difference being measured by a separate instrument to give a check. These numbers yield a conductivity ratio of  $\lambda_+/\lambda_- = 10.3$ , which is rather large for the stated conditions but could be in error by a substantial factor. Without discussing the electric-field strength, Ruhnke [11] also observed the polar conductivities over the ice on Greenland. He reported that  $\lambda_+$  averaged  $3.3 \times 10^{-14} \text{ mho/m}$ , independent of height, whereas, for wind speeds less than 0.5 m/s,  $\lambda_-$  increased from  $0.75 \times 10^{-14} \text{ mho/m}$  at the surface to about  $1.3 \times 10^{-14} \text{ mho/m}$  at a height of 1.8 m. For comparison, we can interpolate a value for the conductivity ratio at 1.5 m of about 2.75.

Neither Pluvinage and Stahl nor Ruhnke seem to have taken pains to prevent contamination of their measurements by the distortion of the earth's field around an elevated and grounded instrument. However, if we assume equal mobilities for positive and negative ions, negligible aerosol density, and a field of 100 V/m at the surface, we can compare their conductivity ratios with the corresponding ratio of small-ion densities of 1.55 computed by Hoppel [3]. Increasing the surface field would increase this ratio by thickening the electrode layer.

The nonturbulent electrode effect in clean air with a nonuniform ionization profile has been studied in an excellent series of papers by Crozier [12,13] and Crozier and Biles [14]. Their observations show that the space charge can reverse from positive in the lowest 10 or 20 cm to negative above, yielding a reversed electrode effect. Good agreement between theory and measurement has been shown by Hoppel [6]. Unfortunately no conductivity measurements were made.